Research Square

Preprints are preliminary reports that have not undergone peer review. They should not be considered conclusive, used to inform clinical practice, or referenced by the media as validated information.

Performance Improvement for Optical OFDM Systems Using Symbol Time Compression

Khaled Ramadan (ramadank637@gmail.com)
Shorouk Academy https://orcid.org/0000-0002-9791-0339

Mohamed S. Elbakry
Institute of Aviation and Technology

Research Article

Keywords: VLC, OFDM, DCO-OFDM, ACO-OFDM and STC

Posted Date: September 30th, 2022

DOI: https://doi.org/10.21203/rs.3.rs-1725212/v1

License: This work is licensed under a Creative Commons Attribution 4.0 International License.
Read Full License

Performance Improvement for Optical OFDM Systems Using Symbol Time Compression

Mohamed S. Elbakry[1] Khaled Ramadan[2]

[1]Department of Electronics and Communications, Institute of Aviation Engineering and Technology (IAET), Giza, Egypt

[2]Department of Electronics and Electrical Communication Engineering, The Higher Institute of Engineering at Al-Shorouk City, Cairo, Egypt

Abstract—**Visible light communication (VLC) is now used to achieve high data rates. Optical-orthogonal frequency division multiplexing (O-OFDM) is a strong technique for intensity modulation and direct detection (IM-DD). Direct current biased O-OFDM (DCO-OFDM) and asymmetrically clipped O-OFDM are two modern O-OFDM systems that operate with IM-DD constraints (ACO-OFDM). Due to severe out of band interference, the DCO-OFDM and ACO-OFDM systems have a high peak to average power ratio (PAPR) and substantial adjacent channel interference (ACI) (OOB). Furthermore, as compared to bipolar OFDM systems, they obtain a greater chance of bit error. The combination of the STC scheme, symbol extension, and pulse shaping signal is presented in this paper for improving the performance of the O-OFDM system without affecting system throughput. This article also decreases the OOB, PAPR, and bit error rate (BER) of DCO-OFDM and ACO-OFDM systems. Further analytical analyses for the proposed systems, such as OOB, PAPR, and computing complexity, are obtained in this paper. The simulation results verify the analytical study of the proposed methods for OOB reduction and PAPR reduction. As compared to typical O-OFDM systems, the proposed shaped STC-DCO-OFDM scheme and the proposed shaped STC-ACO-OFDM scheme lower the OOB by about 40 dB and the PAPR by about 4 dB at the 10^{-3} probability point of the complementary cumulative distribution function (CCDF). The proposed systems outperform existing O-OFDM systems under AWGN for the BPSK modulation scheme in terms of BER, and reduce the computational complexity.**

Index Terms— **VLC, OFDM, DCO-OFDM, ACO-OFDM and STC.**

I. Introduction

Wireless communication data traffic is growing at an exponential rate due to the increasing popularity of smart devices and data-intensive applications and services [1]. To enhance current radio frequency (RF) communication networks, optical wireless communications (OWC) offers a significantly broader and uncontrolled spectrum. Visible light communication (VLC) has lately attracted increased interest as a possible alternative technology due to its unlicensed spectrum resources [2, 3]. Single subcarrier systems such as on-off keying (OOK) and pulse position modulation (PPM) suffer from inter-symbol interference when used for high-data-rate transmission (ISI). As a result, orthogonal frequency division multiplexing (OFDM) is being considered as a viable method of transferring massive volumes of data [4]. Data is frequently sent in VLC via intensity modulation and direct detection (IM/DD) [5, where the electrical signal must be transformed into a real-valued and nonnegative waveform for controlling light emitting diodes] (LEDs).

Traditional OFDM for radio frequency (RF) transmission, which employs the inverse fast Fourier transform (IFFT) to generate complex and bipolar signals, cannot be directly applied to VLC. As a result, suitable optical OFDM converters must be developed. The real-valued output of the IFFT is accomplished by applying a Hermitian symmetry constraint on the frequency-domain signal. Many systems for the O-OFDM system have been developed, including DCO-OFDM and ACO-OFDM [6, 7]. In the DCO-OFDM system, the bipolar real-valued OFDM signals are subjected to a DC bias. Signals below zero must be severely clipped since DC-biased signals cannot totally eliminate negative-valued information.

In ACO-OFDM, only odd frequency subcarriers are used to modulate data, while even frequency subcarriers are set to zero. After IFFT, the time-domain signals are anti-symmetrical. As a result, no information is lost during the clipping step for any negative time-domain signals. Clipping noise in ACO-OFDM occurs exclusively on odd subcarriers of time-domain signals and is orthogonal to

transmission signals. Because clipping noise does not interfere with transmission signals, it may be avoided and thus system performance can be improved. In an ACO-OFDM system, half of the subcarriers broadcast the same signals as the other half of the subcarriers. The bandwidth use of the ACO-OFDM system is around half that of the DCO-OFDM system. As a result, the performance of the ACO-OFDM system can be improved at the price of bandwidth efficiency. Traditional OFDM systems suffer from significant out-of-band (OOB) faults in fourth generation RF transmission. On the other hand, the primary goals of 5G mobile communications are to reduce OOBs and improve spectrum efficiency [8]. However, for downlink systems, the OOB is greatly decreased by utilizing universal filtered-OFDM (UF-OFDM) and improved UF-OFDM (eUF-OFDM) [9], [10]. In addition, O-OFDM systems have a high peak-to-average power ratio (PAPR) [11]. Traditional OFDM systems have a high PAPR in RF communication. It is worth noting that the PAPR has risen in tandem with the number of subcarriers. As a result, the power amplifier (PA) at the transmitter must rely on a back-off, and granular noise in analog-to-digital converters (A/D) at the receiver will rise [11].

There are numerous PAPR reduction techniques for OFDM systems in RF communications [12-14]. Because of the lifetime of LED emitters in IM/DD systems, the effect of PAPR is worse, and big PAPR will compromise the entire interior lighting operation. The PAPR performance of DCO-OFDM and ACO-OFDM systems with the complementary cumulative distribution function (CCDF) calculated and proven by simulations is discussed in [15]. Several techniques for IM/DD optical signals have been proposed, including null subcarrier shifting [16], pilot-symbol assistance [17], and tone injection [18]. ACO-OFDM systems have a lower PAPR than DCO-OFDM systems, albeit at the expense of one-half the spectrum efficiency when employing the same constellation size [4]. In green communication, efficiency, defined as the transmitted data rate per unit of electricity consumed, is becoming increasingly significant [19]. The data rate communicated per bandwidth, also known as spectral efficiency, is a popular statistic for communication systems that may be enhanced by boosting power.

However, when spectral efficiency improves, the energy efficiency may drop. There are many applications for the STC scheme in RF communications, such as ICI reduction for OFDM systems caused by high mobility [20], ICI cancellation using a time inversion scheme (TI) [21]. The STC-shaped scheme for OOB reduction, PAPR reduction, CP elimination, and ISI reduction in wireless channels [22]. In addition to this, the STC-shaped scheme is used for green communication in another way [23]. In the STC scheme [20], the OFDM symbol is compressed by 50% without bandwidth excessing of the system. In this article, this work will be extended into VLC communication systems.

Furthermore, the proposed systems are based on the STC process, symbol extension, and pulse shaping functions at the transmitter, and then combining processes only at the receiver. The STC scheme is implemented by using Walsh spreading code for signal spreading at the transmitter and then the combining and symbol mapping are applied for symbol compression. Hence, the STC scheme enables us to save one-half of the symbol duration, which will be exploited for symbol extension without any effect on the system throughput compared to the traditional DCO-OFDM and ACO-OFDM systems. Finally, the pulse shaping function based on raised cosine is applied for the transmitted symbol in the time domain at the transmitter. The raised cosine function has the complementary property during the transmission of the symbol. On the other hand, the combing process is applied at the receiver. The combing process is achieved by the summing of the useful part and the extended part. Matlab simulations are conducted to confirm the OOB, the PAPR and BER analysis for the proposed STC-DCOOFDM and the proposed STC-ACOOFDM schemes compared to the traditional DCO-OFDM and traditional ACO-OFDM systems. The contributions to these articles are itemized as follows:

1) The OOB reduction of the DCO-OFDM and ACO-OFDM systems will reduce adjacent channel interference (ACI).
2) The PAPR reduction of the traditional O-OFDM systems.
3) The OOB reduction and the PAPR reduction are derived analytically.

4) The improvement in BER performance is under AWGN for the BPSK scheme.

5) The computational complexity of the proposed schemes is derived.

The following describes the structure of this document. The system models for DCO-OFDM and ACO-OFDM systems are described in Section II. Sections III and IV address the suggested shapes STC-DCO-OFDM and STC-ACOOFDM, as well as the performance analysis and comparison of the proposed systems. Section V contains simulation findings that are used to validate the theoretical analysis. Finally, in Section VI, we describe our results.

II. System Model

In this section, the DCO-OFDM and ACO-OFDM system models are explained in the following subsections.

A. DCO-OFDM SYSTEM MODEL

In traditional OFDM, the transmitted signal is complex and bipolar in radio frequency (RF) communication. In VLC communication systems IM/DD transmit the signals in form of optical power. Provided that in VLC systems, the signal must be transmitted real and unipolar due to the usage of IM/DD. To obtain real valued signal, OFDM subcarriers are rearranged before IFFT operation by using Hermitian symmetry. In addition to this, to get unipolar signal a direct current (DC) bias is added to the transmitted signal in order to achieve DCO-OFDM. The block diagram of DCO-OFDM system is presented in Figure 1.

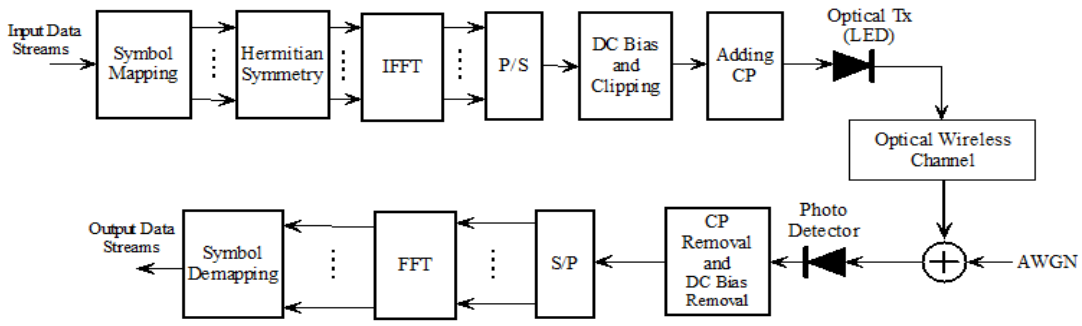

Figure 1. Block diagram of DCO-OFDM System [24].

In DCO-OFDM, the Hermitian symmetry will be applied to maintain the signal obtained after IFFT is real-valued. This equation satisfies the following conditions [25, 26],

$$X_k = X_{2N-k}^{*}\,, \qquad k = 0, 1, \dots\dots, N-1 \tag{1}$$

$$X_0 = X_N = 0 \tag{2}$$

For $2N$ subcarriers, the Hermitian symmetry property is defined in [27] as:

$$\{Z_k^{DCO}\}_{k=0}^{2N-1} = [0 \quad \{X_k\}_{k=1}^{N-1} \quad 0 \quad \{X_k^{*}\}_{k=1}^{N-1}] \tag{3}$$

After IFFT, the time domain sample points of the DCO-OFDM system will be obtained as:

$$z_n^{DCO} = \frac{1}{2N}\sum_{k=0}^{2N-1} Z_k^{DCO} \exp\left(\frac{j2\pi kn}{N}\right).\ 0 \le n \le 2N-1 \tag{4}$$

Until recently, the bipolar OFDM signal has been transformed to real numbers, but it may contain negative values, making it unsuitable for intensity modulation (IM). To sustain non-negative signals, a very high DC-bias B_{dc} is required [25, 26]. Because of the high DC-bias, the optical energy per bit to single-sided noise power spectral density $\left(E_{b(opt)}/N_0\right)$ is quite high. As a result, the DCO-OFDM approach will be inefficient in terms of optical power. A DC bias B dc proportionate to the root-square of the electric power (σ_x) can be used to prevent a bulky DC bias while minimizing the required optical power, as demonstrated below:

$$B_{dc} = q\sigma_x = k\sqrt{E\{z_n^2\}} \tag{5}$$

where q represents the clipping factor and $\sigma_x^2 = E\{z_n^2\}$ is the variance of signal z_n [25, 26].

$$B_{dc} = 10\,log_{10}(q^2+1)\ dB \tag{6}$$

After DC biasing, the transmitted signal z_n, becomes

$$z_O)_n = z_n + B_{dc} \tag{7}$$

After DC biasing, some samples of the signal may quiet be negative. Thus, clipping process must be applied to ensure that all negative samples are set to zero as follows:

$$z_{DCO})_n = \begin{cases} z_O)_n, & \text{if } z_O)_n \ge 0 \\ 0, & \text{if } z_O)_n < 0 \end{cases} \tag{8}$$

As a result, the hard clipping leads to a clipping noise that deteriorate the BER performance. Thus, the unipolar signal of DCO-OFDM can be stated as:

$$z_{DCO})_n = z_n + n_c(B_{dc}) + B_{dc} \tag{9}$$

The clipping noise component is denoted by $n_c(B_{dc})$. The inferiority of DC bias leads in a greater number of subcarriers that are clipped. As a result, clipping noise is determined by the additional DC bias B_{dc}. The DCO-OFDM systems have several drawbacks like dropping one-half of the system throughput and, large optical power consumption.

B. ACO-OFDM SYSTEM MODEL

Odd subcarriers convey information in ACO-OFDM, while even subcarriers are set to zero. All of the even IFFT inputs in DCO-OFDM are set to zero. As a result, the total number of subcarriers in ACO-OFDM is 4N. [27] describes the placement of complicated symbols on SCs.

$$\{Z_k^{ACO}\}_{k=0}^{4N-1} = [0\ X_0\ 0\ \ X_1 \dots\ 0\ \ X_{N-1} 0\ X_{N-1}^* 0 \dots X_1^*\ 0\ X_0^*] \tag{10}$$

After IFFT, the time domain signal is given in [27] as:

$$z_n^{ACO} = \frac{1}{4N} \sum_{k=0}^{4N-1} Z_k^{ACO} \exp\left(\frac{j2\pi kn}{N}\right), \qquad 0 \le n \le 4N-1 \tag{11}$$

The Hermitian symmetry and IFFT result in a real time domain signal and has the asymmetry property given in [24] as:

$$z_n^{ACO} = -z_{n+2N}^{ACO}, \qquad 0 \le n \le N \tag{12}$$

The ACO-OFDM signal is zero clipped to send the positive part. Hence, the asymmetry of x_n clipping does not leads to information loss. At the receiver side, the odd subcarriers are only recovered

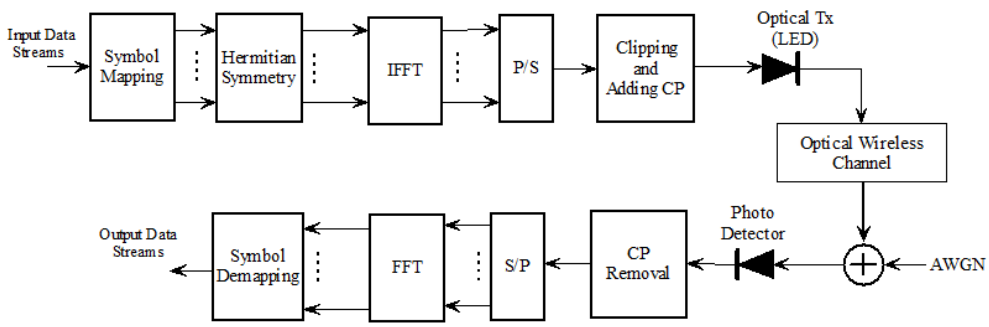

Figure 2. Block diagram of ACO-OFDM system [24].

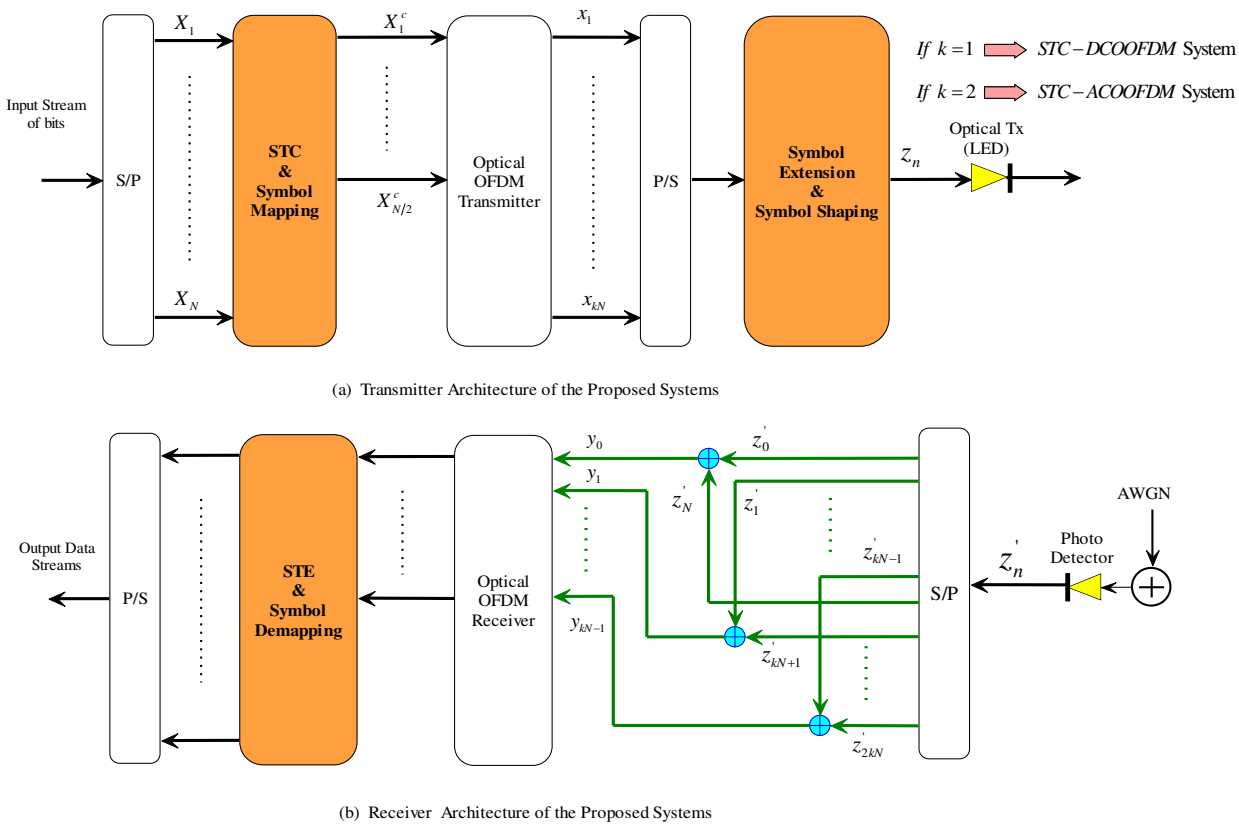

Figure 3. Block diagram of the proposed Systems**.**

III. The Proposed Systems

The proposed techniques for improving the performance of DCO-OFDM and ACO-OFDM systems are described in this section. Figure 3 depicts the transmitter and receiver structures for the proposed systems.

A. The PROPOSED SHAPED STC-DCO-OFDM

The proposed scheme is fundamentally based on the STC system, symbol extension, and signal shaping at the transmitter terminal. At the receiver terminal, the combining and the symbol time expansion (STE) processes are performed. Using the STC system, the OFDM symbol is compressed into one half [20- 22]. Hence, the number of subcarriers become $N/2$. Hence, the frequency domain of the modulated signal after the STC scheme becomes

$$X_k^c = \left[X_0^c, X_1^c, \dots\dots, X_{N/2-1}^c\right] \tag{13}$$

Where X_k^c denotes the modulated symbol after the STC process. Consequently, the STC-DCOOFDM signal after Hermitian symmetry operation can be presented as follows:

$$X_k^{DCO} = \left[\underbrace{0}_{X_0}, X_0^c, X_1^c, \dots, \underbrace{0}_{X_{N/2}}, X_{N/2+1}^*, \dots, X_1^{c*}, X_0^{c*} \right] \tag{14}$$

From equation (14), the number of transmitted signals becomes N instead of $2N$ compared to the traditional DCO-OFDM system. Hence, the time domain sample of x_n^{DCO} is given by

$$x_n^{DCO} = \frac{1}{N} \sum_{k=0}^{N-1} X_k^{DCO} \exp\left(\frac{j2\pi kn}{N}\right), \qquad 0 \le n \le N-1 \tag{15}$$

Now, the Hermitian symmetry for generation real valued is achieved without loss of the spectral efficiency as shown in Figure 4.

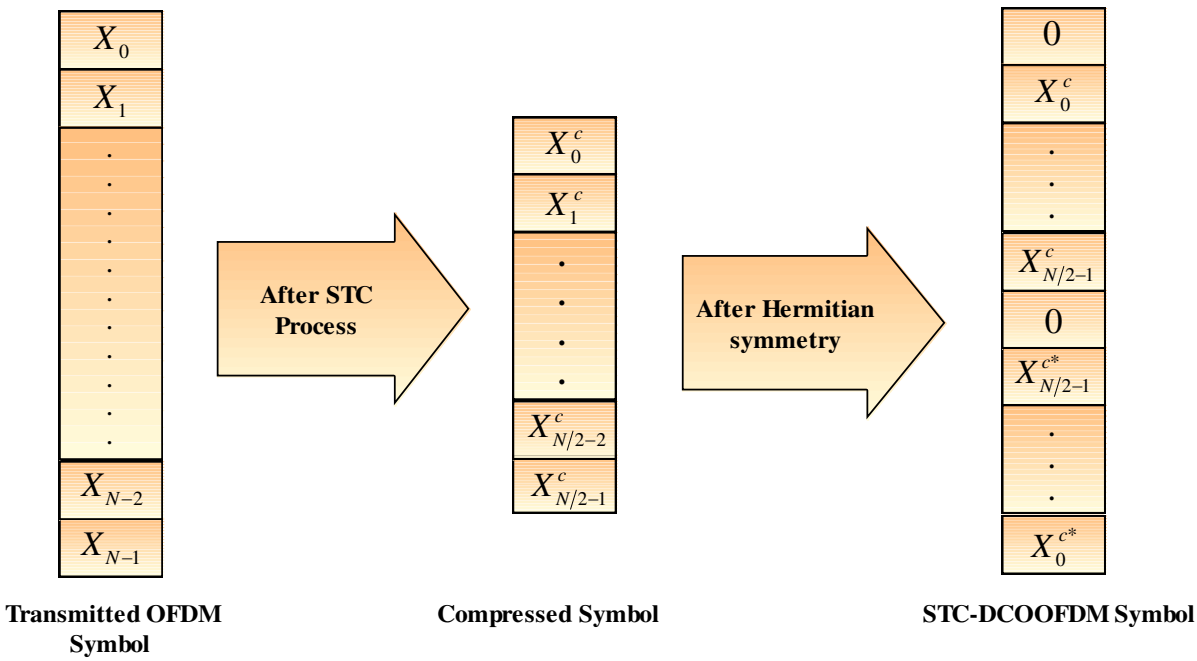

Figure 4. The DCO-OFDM Combined with STC Process.

As a result, the joint STC process with the DCO-OFDM system increases spectral efficiency. After symbol extension, the time domain is given as follows:

$$x_n^{DCO} = \frac{1}{N} \sum_{k=0}^{N-1} X_k^{DCO} \exp\left(\frac{j2\pi kn}{N}\right), \qquad 0 \le n \le 2N-1 \tag{16}$$

The shaping process is accomplished using the raised cosine function and is given by [30] as:

$$p_n = \frac{1}{2}\left[1 - \cos\left(\frac{2\pi n}{N}\right)\right], \qquad 0 \le n \le 2N - 1 \tag{17}$$

As illustrated in Figure 5, the pulse shaping function is symmetric and has a complimentary concept in the first and second halves.

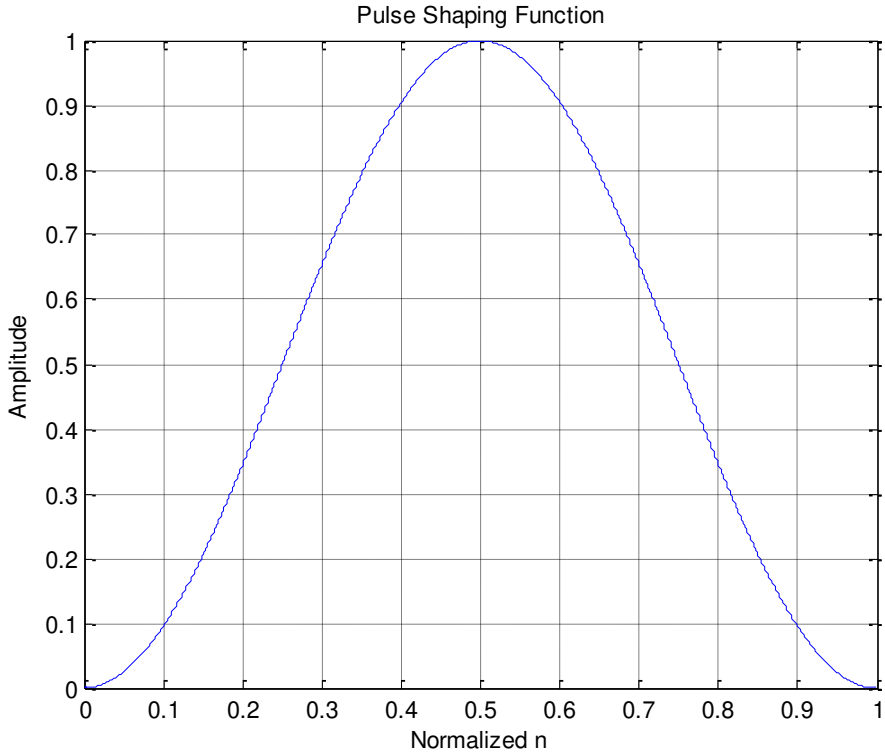

Figure 5. The pulse shaping function.

Furthermore, the transmitted DCO-OFDM symbol turns out to be:

$$z_n^{DCO} = \frac{1}{2N}\sum_{k=0}^{N-1} X_k^{DCO} \exp\left(\frac{j2\pi kn}{N}\right)\left[1 - \cos\left(\frac{2\pi n}{N}\right)\right], \quad 0 \le n \le 2N - 1 \tag{18}$$

At the receiver side, the received signal is given by:

$$z'_n = z_n^{DCO} + w_n, \qquad 0 \le n \le 2N - 1 \tag{19}$$

After combining process, the received signal becomes:

$$y_n^{DCO} = z'_n + z'_{N+n}, \qquad 0 \le n \le N - 1 \tag{20}$$

After DC bias removal and FFT operation, the received signal can be expressed as:

$$Y_k^{DCO} = \sum_{n=0}^{N-1} y_n^{DCO} \exp\left(-\frac{j2\pi kn}{N}\right), \qquad 0 \le k \le N - 1 \tag{21}$$

Finally, the STE process is applied for recovered the transmitted bits [20- 22].

B. The PROPOSED SHAPED STC-ACOOFDM SCHEME

The proposed shaped STC-ACOOFDM is also based on the STC process in Figure 3. The transmitted data is compressed by one-half using the STC process. After that, the Hermitian symmetry operation for equation (13) becomes as:

$$X_k^{ACO} = \left[\underbrace{0}_{X_0^{ACO}}, X_0^c, 0, \dots, X_{N/2-1}^c, \underbrace{0}_{X_N^{ACO}}, X_{N/2-1}^{c*}, \dots, 0, X_0^{c*}, \underbrace{0}_{X_{2N}^{ACO}} \right] \tag{22}$$

After the IFFT, the time domain sample of x_n^{ACO} is given by

$$x_n^{ACO} = \frac{1}{2N} \sum_{k=0}^{2N-1} X_k^{ACO} \exp\left(\frac{j2\pi kn}{N}\right) 0 \le n \le 2N-1 \tag{23}$$

However, the proposed STC-ACOOFDM procedures is illustrated in Figure 6

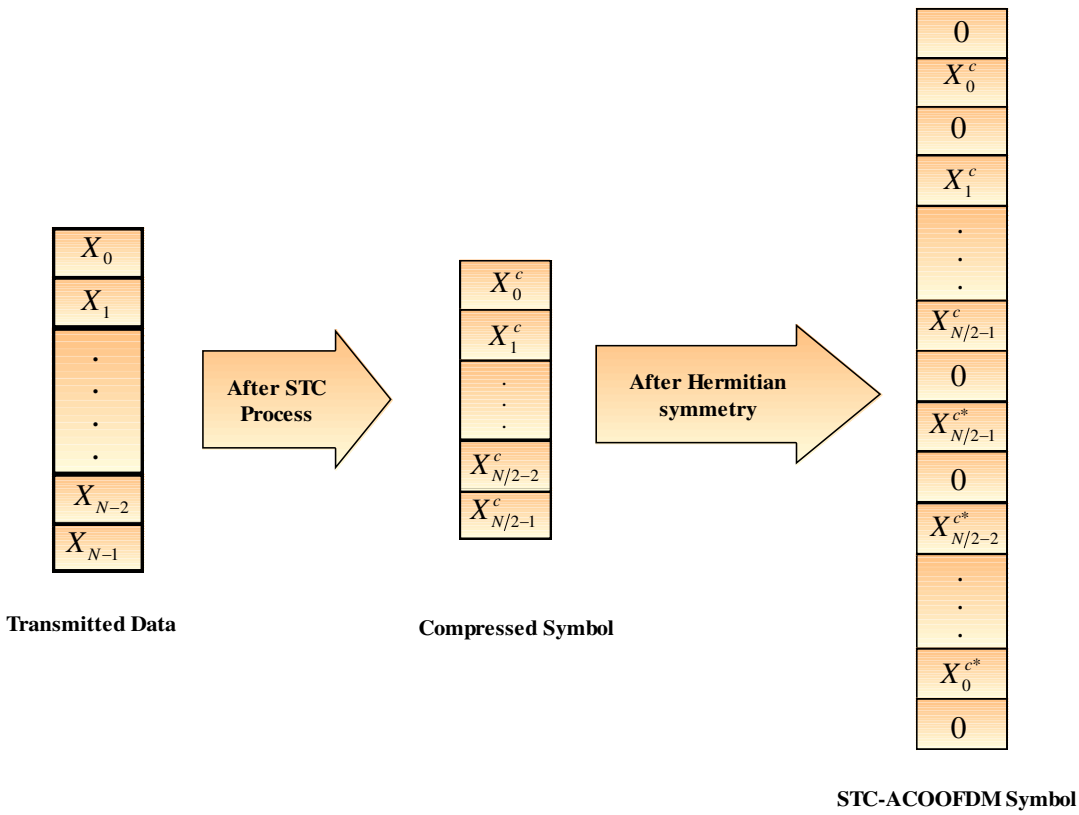

Figure 6. The ACO-OFDM Combined with STC Process.

Therefore, Hermitian symmetry generates real value and is achieved with higher spectral efficiency than traditional ACO-OFDM. After symbol extension and pulse shaping function in equation (17), the transmitted ACO-OFDM symbol turns out to be:

$$z_n^{ACO} = \frac{1}{4N}\sum_{k=0}^{2N-1} X_k^{ACO} \exp\left(\frac{j2\pi kn}{N}\right)\left[1-\cos\left(\frac{2\pi n}{N}\right)\right] \quad 0 \le n \le 4N-1 \tag{24}$$

At the receiver side, the received signal is given by:

$$z_n'' = z_n^{ACO} + w_n, \qquad 0 \le n \le 4N-1 \tag{25}$$

After combining process, the received signal becomes:

$$y_n^{ACO} = z_n'' + z_{N+n}'', \qquad 0 \le n \le 2N-1 \tag{26}$$

After FFT operation, the received signal can be given by:

$$Y_k^{ACO} = \sum_{n=0}^{N-1} y_n^{ACO} \exp\left(-\frac{j2\pi kn}{N}\right) \quad 0 \le k \le N-1 \tag{27}$$

Finally, the data bits are recovered by using the STE process as in the previous section. Figure 7 shows all the procedures for the proposed shaped STC-DCOOFDM and the proposed shaped STC-ACOOFDM systems by flowchart.

IV. Performance Analysis and Comparison

This section compares the proposed STC-DCOOFDM and STC-ACOOFDM schemes to standard DCO-OFDM and ACO-OFDM systems using mathematical analysis and comparison. These investigations focus on the fundamentals of spectral efficiency, OOB, PAPR, and computational complexity.

A. SPECTRAL EFFICIENCY

The spectral efficiency of the proposed systems will be illustrated throughout this section. The spectral efficiency will be introduced analytically and through simulation.

1) The proposed shaped STC-DCOOFDM system

The achieved data rate for the DCO-OFDM system is given in [28] as:

$$\eta_{DCO} = \left(\frac{N-1}{2N+N_{cp}}\right) B\, log_2 M \;\; bits/sec, \tag{28}$$

where B is the bandwidth, N_{cp} is the number of guard subcarriers in the CP, and M is the modulation order. Figure 8 depicts the typical DCO-OFDM system's time samples of the bipolar OFDM symbol and the time signal after clipping.

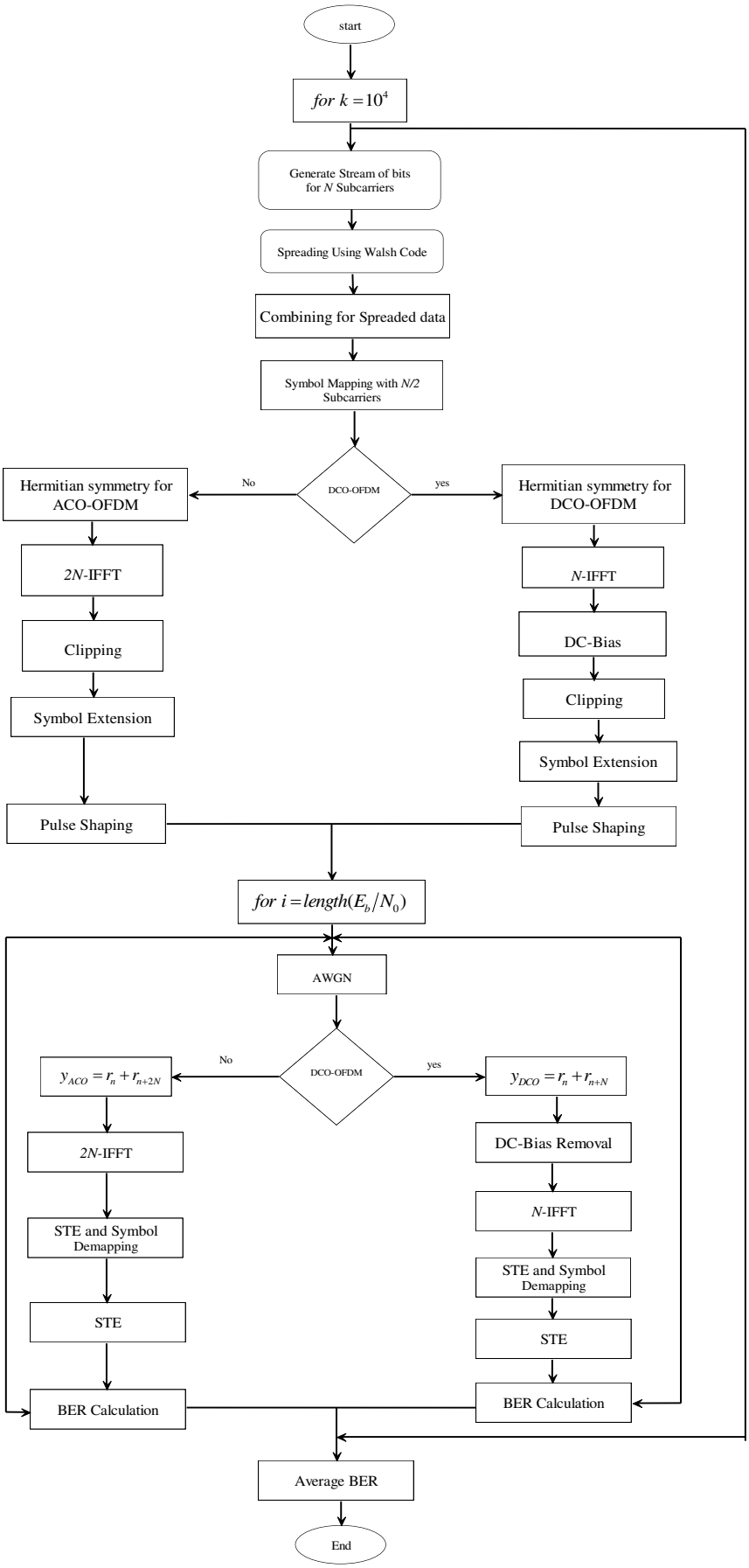

Figure 7. Flow chart of the proposed systems.

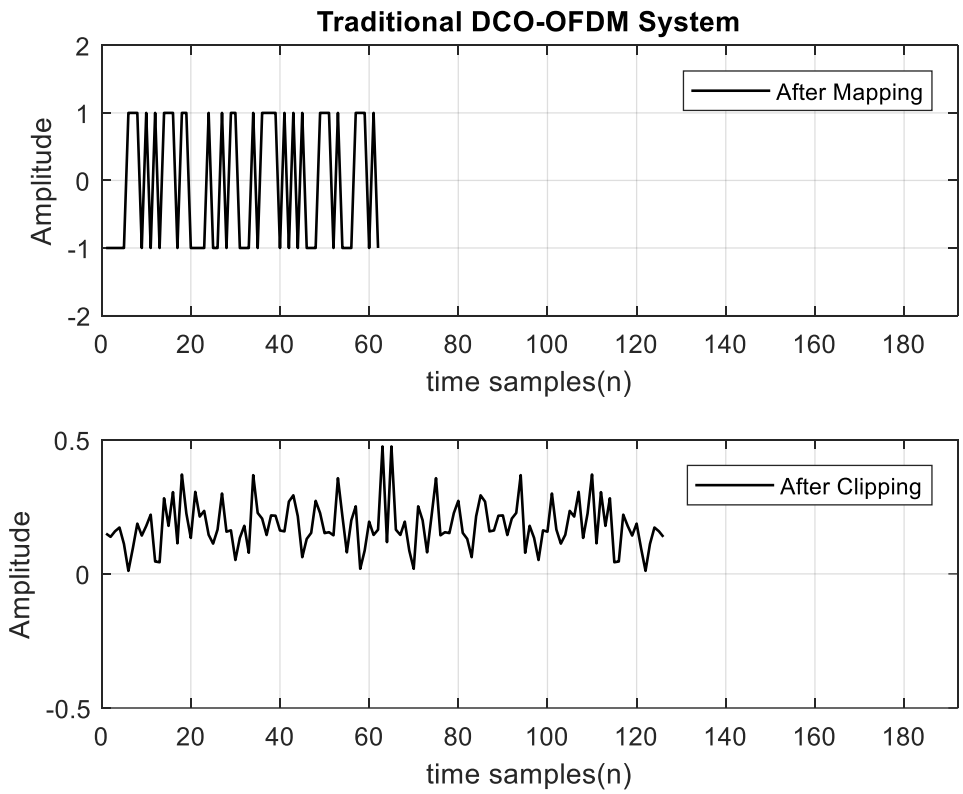

Figure 8. Time-domain signal for DCO-OFDM system.

After the STC process, the information signal can be conveyed in half duration instead. Thus, the achieved data rate for the proposed STC-DCOOFDM system is given by:

$$\eta_{STC-DCO} = \left(\frac{N_c - 1}{2N_c + N_{cp}}\right) B \log_2 M \ \ bits/\text{sec}, \tag{29}$$

It is noted that the bit rate of the proposed STC-DCO-OFDM system is doubled. However, the proposed STC-DCO-OFDM can transmit $2N$ data through N instead as compared to the traditional DCO-OFDM system as shown in Figure 9. It is shown from Figure 10, the whole bipolar OFDM symbol is compressed into one-half and then, the whole symbol of the proposed STC-DCOOFDM system after clipping with the size of N samples. Hence, the DCO-OFDM using the STC process doubles the system throughput. After symbol repetition and pulse shaping, the spectral efficiency will be the same as the traditional DCO-OFDM system as shown in Figure 10.

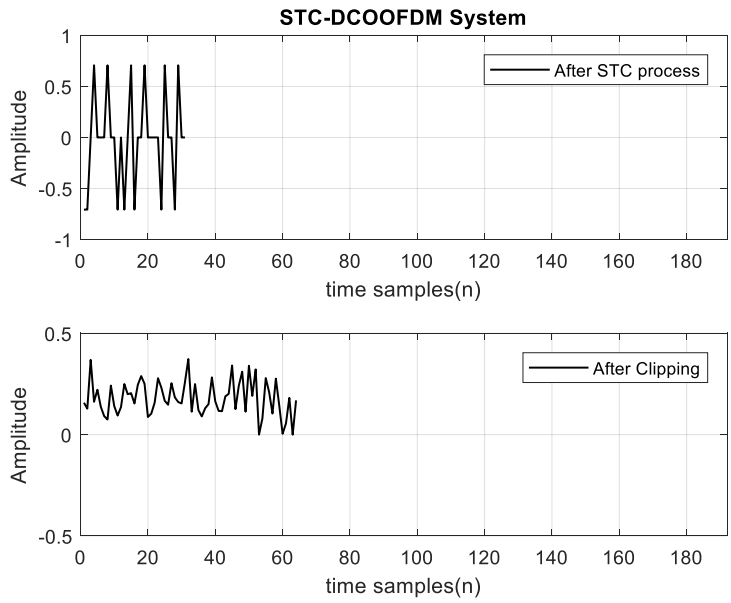

Figure 9. Time-domain signal for DCO-OFDM using the STC.

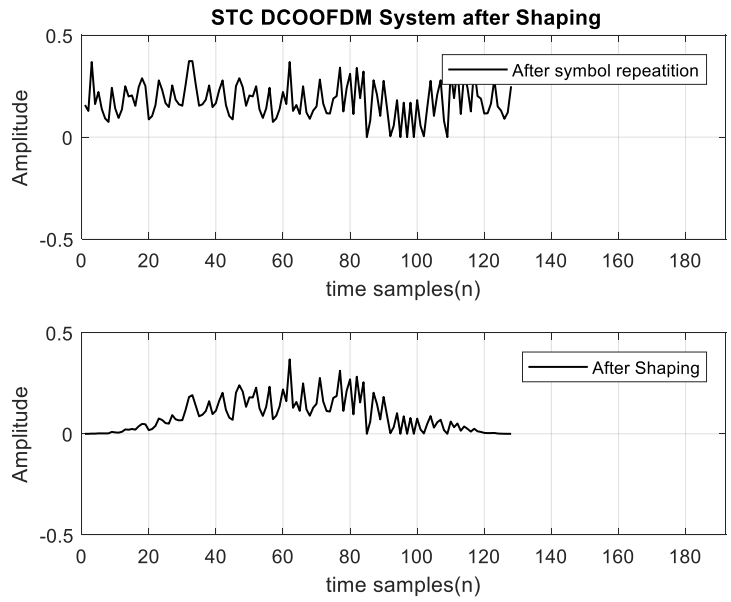

Figure 10. The proposed shaped STC-DCOOFDM symbol.

It is illustrated in Figure 10, the proposed shaped STC-DCO-OFDM has the same spectral efficiency as the traditional DCO-OFDM system.

2) The proposed shaped STC-DCOOFDM system

The accomplished data rate for the traditional ACO-OFDM system is given by:

$$\eta_{ACO} = \left(\frac{2N-1}{4N+N_{cp}}\right) B \log_2 M \ \ bits/sec, \tag{30}$$

It is shown from Figure 11, the time samples for the traditional ACO-OFDM system after clipping is extended to $4N$. This means that to prepare the ACO-OFDM symbol, the system throughput will be reduced to one-quarter.

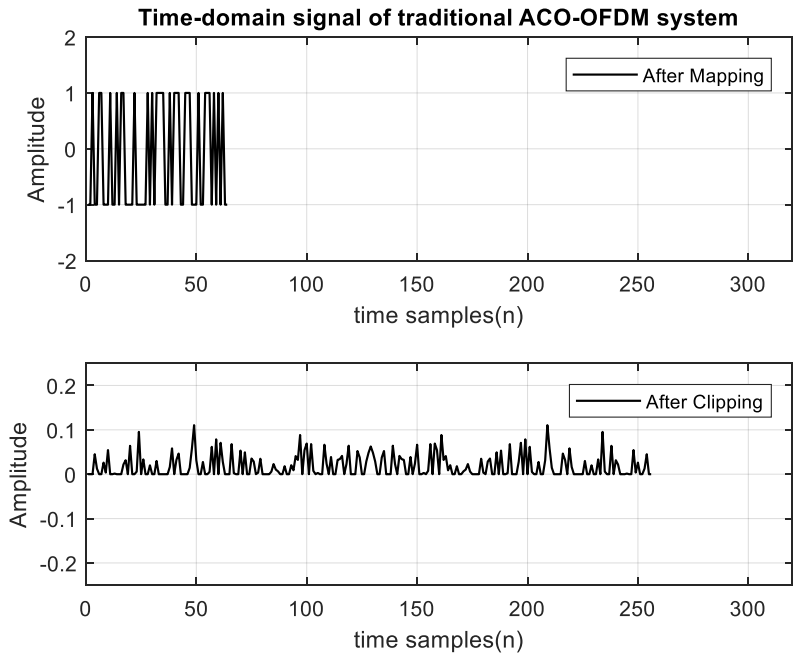

Figure 11. Time-domain signal for ACO-OFDM system.

After the STC process, the achieved data rate for the ACO-OFDM system using the STC process is given by:

$$\eta_{STC-ACO} = \left(\frac{2N_c - 1}{4\,N_c + N_{cp}}\right) B\, log_2\, M \;\; bits/sec, \qquad (31)$$

Furthermore, the bit rate of the ACO-OFDM system using the STC process will be doubled. Thus, the ACO-OFDM symbol using the STC process is transmitted in $2N$ instead of $4N$ as compared to traditional ACO-OFDM as shown in Figure 12.

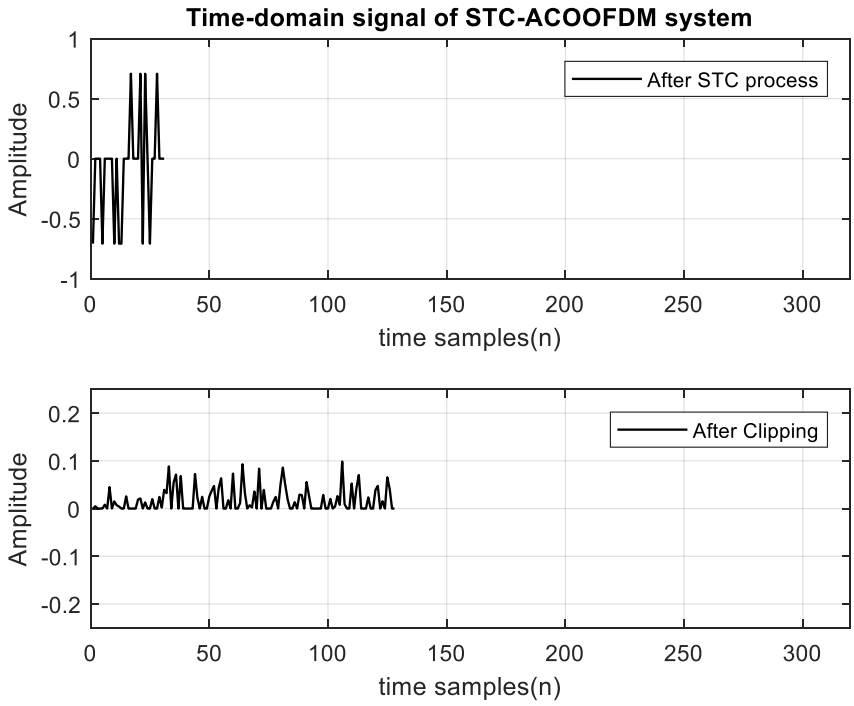

Figure 12. Time-domain signal for ACO-OFDM using the STC.

Figure 12 shows that the ACO-OFDM symbol length is $2N$ using the STC process. Hence, an ACO-OFDM system using the STC process increases the system throughput to be $N/2$ instead $N/4$ compared to a traditional ACO-OFDM system. After symbol repetition and pulse shaping, the spectral efficiency will be the same as the traditional ACO-OFDM system as shown in Figure 13.

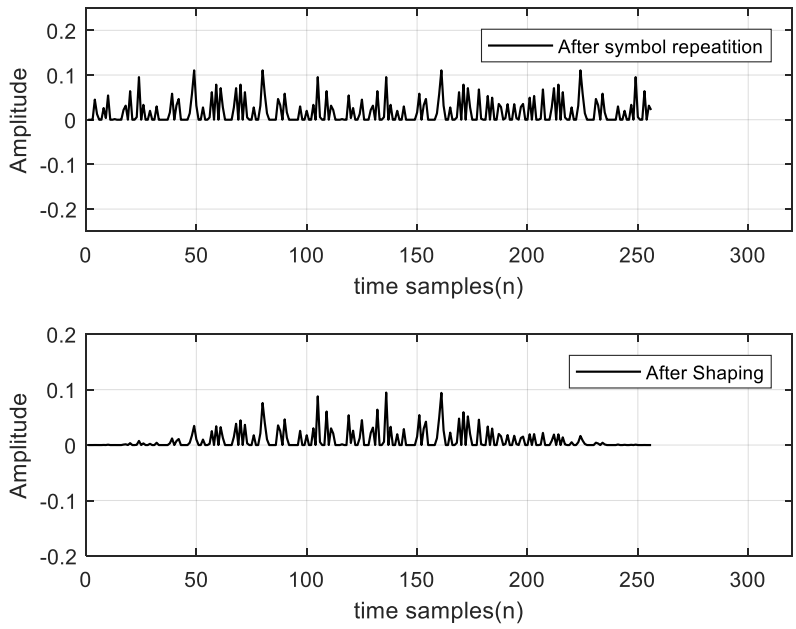

Figure 13. The proposed shaped STC-ACOOFDM symbol.

Figure 13 shows that the proposed shaped STC-ACO-OFDM system has the same spectral efficiency as the traditional ACO-OFDM system. In the next subsection, the OOB of the proposed schemes is analyzed and evaluated.

B. OOB REDUCTION

1) *The proposed shaped STC-DCOOFDM system*

Consider an O-OFDM symbol after the STC process is defined as $X_n,\ n = 0,1, \dots \dots \dots, N/2 - 1$. The O-OFDM signal after Hermitian symmetry and IFFT can be expressed in [29] as

$$x(t) = \sum_{n=0}^{N-1} X_{n,k}\, e^{j2\pi n\Delta f t}, \qquad 0 \le t \le T, \tag{32}$$

Where Δf is subcarrier spacing. After symbol extension and pulse shaping, the O-OFDM symbol can be expressed as:

$$x_p(t) = p(t) \sum_{n=0}^{N-1} X_{n,k}\, e^{j2\pi n\Delta f t}, \qquad 0 \le t \le 2T \tag{33}$$

where $p(t)$ is the pulse shaping function. The autocorrelation function of the transmitted signal $R_x(\tau)$ is obtained in [29] as:

$$R_x(\tau) = E\{x_p(t+\tau)x_p(t)^*\} = p(t+\tau)p^*(t) \sum_{n=0}^{N-1} e^{j2\pi n\Delta f \tau} \tag{34}$$

The power spectral density (PSD) will be obtained by the Fourier transform (FT) of the autocorrelation function. This can be expressed as

$$S(f) = \int E\left\{\bar{R}_x(\tau) \sum_{n=0}^{N-1} e^{j2\pi n\Delta f \tau}\right\} e^{j2\pi n\Delta f \tau} d\tau \tag{35}$$

where

$$\bar{R}_x(\tau) = \frac{1}{T}\int_0^T p(t+\tau)p^*(t)\, dt \tag{36}$$

We have

$$S(f) = \frac{1}{T}\sum_{n=0}^{N-1}\{P[(f - n\Delta f)T]\}^2 \tag{37}$$

where $P(f)$ is the FT of the pulse shaping function. The pulse shaping function that is used during the interval $2T$ for the transmitted optical OFDM signal can be expressed as follows:

$$p(t) = \frac{1}{2}\left[1 - \cos\left(\frac{2\pi t}{4T}\right)\right] \operatorname{rect}\left(\frac{t}{4T}\right) \tag{38}$$

The PSD of optical OFDM signal multiplied by a pulse shaping function is given by:

$$S(f) = \frac{1}{T}\sum_{n=0}^{N-1}\{P[(f - n\Delta f)T]\}^2 \tag{39}$$

The frequency domain of pulse shaping function (see proof in Appendix) can be get by FT as follows:

$$S(f) = 4T\sum_{n=0}^{N-1}\left\{\operatorname{sinc}[2(f - n\Delta f)]\frac{\cos[2\pi T(f - n\Delta f)]}{[1 - T^2(f - n\Delta f)^2]}\right\}^2 \tag{40}$$

The PSD of the proposed shaped STC-DCO-OFDM system in comparison with the traditional DCO-OFDM system is offered in Figure 14. These results were obtained with 1024 subcarriers and 10^4 symbols.

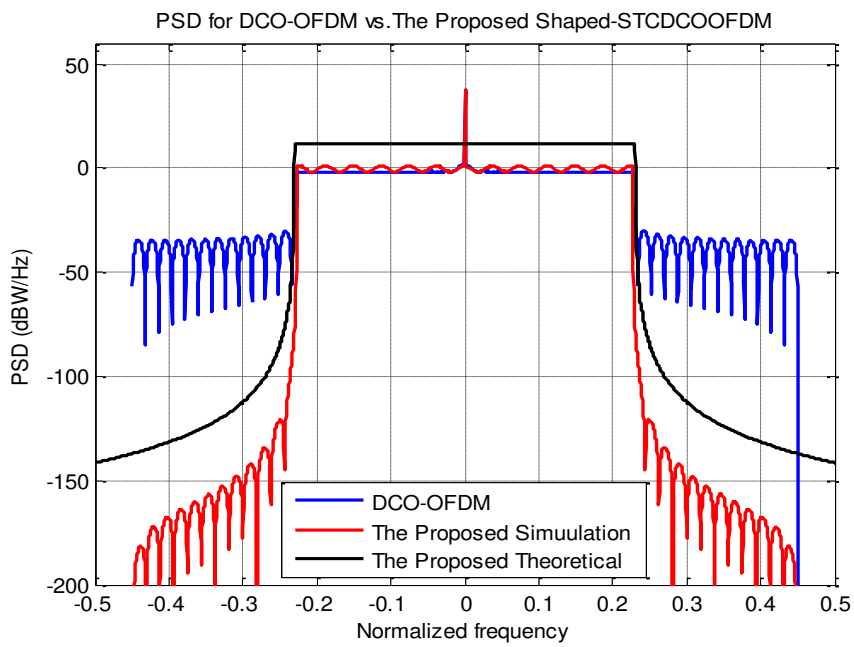

Figure 14. PSD of the proposed shaped STC-DCO-OFDM system.

It is observed from Figure 14 that the proposed system has lower side lobes compared to the traditional DCO-OFDM systems. Hence, the reduction of OOB via the proposed shaped STC-DCO-

OFDM system by about 80 dB. Finally, there is no significant variance noticed between theoretical and simulated results.

2) The proposed shaped STC-ACOOFDM system

Similarly, the pulse shaping function in equation (38) for the transmitted ACO-OFDM signal can be altered as:

$$p(t) = \frac{1}{2}\left[1 - \cos\left(\frac{2\pi t}{8T}\right)\right] \mathrm{rect}\left(\frac{t}{8T}\right) \tag{41}$$

After some manipulation, the PSD of for the proposed shaped STC-ACOOFDM is given as follows:

$$S(f) = 4T \sum_{n=0}^{N-1} \left\{ \mathrm{sinc}[4(f - n\Delta f)] \frac{\cos[4\pi T(f - n\Delta f)]}{[1 - T^2(f - n\Delta f)^2]} \right\}^2 \tag{42}$$

The PSD of the proposed shaped STC-ACOOFDM compared with ACO-OFDM system for 1024 subcarriers and 10^4 symbols is available in Figure 15.

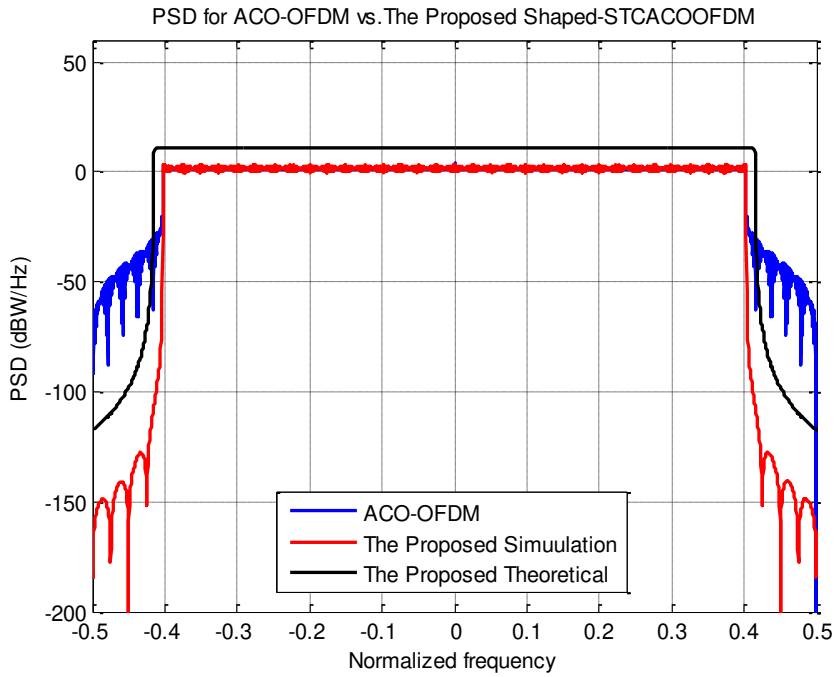

Figure 15. PSD of the proposed shaped STC-ACO-OFDM system.

It is perceived from Figure 14 and Figure 15 that the ACO-OFDM system needs about twice the bandwidth of DCO-OFDM for the same amount of transmitted information. In addition to this, the proposed systems reduce OOB by about 40 dB compared to the traditional ACO-OFDM system. As a result, the OOB reduction will reduce the ACI and the AWGN, which improves the BER

performance. Finally, it is noticed that theoretical and simulated results are closest to each other. The PAPR reduction and power saving of the proposed systems are derived in the next subsection.

C. PAPR REDUCTION

1) The proposed shaped STC-DCOOFDM system

The mathematical relationship of the PAPR for The maximum power to average power ratio of an OFDM signal is expressed as:

$$\xi^{DCO} = \frac{\max\limits_{n \in [0,2N-1]} \{|x_n|^2\}}{\mathrm{E}\{|x_n|^2\}} \tag{43}$$

Assume X_k is an i.i.d. random variable (RV) with zero mean and variance $\sigma^2 = E\{|X_k|^2\}$. It follows that each frame is i.i.d. the average power of the proposed STC-DCOOFDM is given as:

$$\mathrm{E}\{|z_n|^2\} = \frac{1}{4N^2}\mathrm{E}\left\{\left|\sum_{k=0}^{2N-1} Z_k^{DCO} \exp\left(\frac{j2\pi kn}{N}\right)\right|^2\right\} \tag{44}$$

Assume $Z_k^{DCO} = 1$ over DCO-OFDM symbol. Thus, the average power for DCO-OFDM symbol is given as follows:

$$\mathrm{E}\{|z_n|^2\} = \frac{1}{2N} \tag{45}$$

The peak value z_0 is given as $z_0 = \frac{1}{2N}\sum_{k=0}^{2N-1} 1 = 1$ and the peak power $= |z_0|^2 = 1$. Thus, the PAPR for DCO-OFDM system is $\xi^{DCO} = 2N$. Hence, the proposed shaped STC-DCOOFDM symbol is obtained as follows:

$$z_n = z_n p_n = z_n \frac{1}{2}\left[1 - \cos\left(\frac{\pi n}{N}\right)\right], 0 \le n \le 2N-1 \tag{46}$$

Due to the complementary of pulse shaping and the symbol extension, the summation is always equal to N and the peak value z_0 is obtained

$$z_0 = \frac{1}{N}\sum_{k=0}^{N-1} 1\ \frac{1}{2}\left[1 - \cos\left(\frac{\pi n}{N}\right)\right] = \frac{1}{2} \tag{47}$$

As a result, the suggested shaped STC-DCOOFDM has a peak power of 14. As a result, the average power of the suggested shaped STC-DCO-OFDM system is as follows:

$$\mathrm{E}\{|z_n|^2\} = \frac{1}{4}\mathrm{E}\left\{z_n\left[1-\cos\left(\frac{\pi n}{N}\right)\right]^2\right\} = \frac{3}{8N} \tag{48}$$

As a result, the PAPR for the proposed system can be obtained as follows:

$$\xi^{\text{Shaped STC-DCO}} = \frac{2}{3}N \tag{49}$$

2) The proposed shaped STC-ACOOFDM system

Likewise, the PAPR is defined over ACO-OFDM frame interval as

$$\xi^{ACO} = \frac{\max\limits_{n\in[0,4N-1]}\{|x_n|^2\}}{\mathrm{E}\{|x_n|^2\}} \tag{50}$$

The average power of the ACO OFDM system is given as:

$$\mathrm{E}\{|z_n|^2\} = \frac{1}{16N^2}\mathrm{E}\left\{\left|\sum_{k=0}^{4N-1} Z_k^{ACO}\exp\left(\frac{j2\pi kn}{N}\right)\right|^2\right\} \tag{51}$$

Assume $Z_k^{ACO} = 1$ over ACO-OFDM symbol. Thus, the average power for ACO-OFDM symbol is $1/4N$ and the peak power is also 1. Thus, the PAPR for ACO-OFDM system is $\xi^{ACO} = 4N$. Furthermore, the proposed shaped STC-ACOOFDM symbol is obtained as follows:

$$z_n = z_n p_n = z_n\frac{1}{2}\left[1-\cos\left(\frac{\pi n}{2N}\right)\right] \quad 0 \le n \le 4N-1 \tag{52}$$

Similarly, the peak power and the average power are $1/4$ and $3/8N$. Thus, the PAPR for the proposed shaped STC-ACOOFDM system is given

$$\xi^{\text{Shaped STC-DCO}} = \frac{2}{3}N \tag{53}$$

Consequently, the proposed shaped STC-DCOOFDM and the proposed shaped STC-ACOOFDM reduce the PAPR by one-third (or -4.77 dB).

D. COMPUTATIONAL COMPLEXITY

The computational complexity of the suggested systems is examined in this section. The complexity is calculated as the total amount of arithmetic operations necessary at the transceiver, either additions or multiplications. The computational complexity of transmitters for the recommended designs is shown in Table I. As can be shown, the suggested approaches reduce the system's computational complexity when compared to typical DCO-OFDM and ACO-OFDM systems.

TABLE I

Computational complexity of the proposed schemes

System Type	No. of real multiplications	No. of real additions
DCO-OFDM [30]	$N \log_2 2N$	$2N \log_2 2N$
Proposed shaped STC-DCOOFDM	$N/2 \log_2 N + 2N$	$N \log_2 N$
ACO-OFDM [31]	$2N \log_2 4N$	$4N \log_2 4N$
Proposed shaped STC-ACOOFDM	$N \log_2 2N + 4N$	$N \log_2 N$

Hence, the proposed STC-DCOOFDM and the proposed STC-ACOOFDM schemes will reduce multiplication operations by about 64 %. On the other hand, addition operations will be reduced by about 45.5% and 20.8% by the proposed schemes, respectively

V. Numerical Results

The performance of the proposed approach is investigated in terms of PAPR reduction and improvement of BER. The simulation is accomplished using Matlab software for 10^4 optical OFDM frames of BPSK symbols. The number of subcarriers used in the simulation is 1024. In VLC communication systems, the communication channels are almost line of sight (LOS). Hence, the AWGN channel will be considered for the BER performance of the proposed systems. The PAPR reduction performance is assessed using the CCDF of the PAPR. Figure 16 and Figure 17 show the CCDF of the PAPR for the proposed systems compared to the conventional systems, respectively. As shown in Figure 16, the PAPR performance of the proposed shaped STC-DCO-OFDM scheme

outperforms that of the conventional DCO-OFDM system. When CCDF=10^{-1}, the PAPR of the proposed scheme is less than the conventional DCO-OFDM systems by about 3 dB.

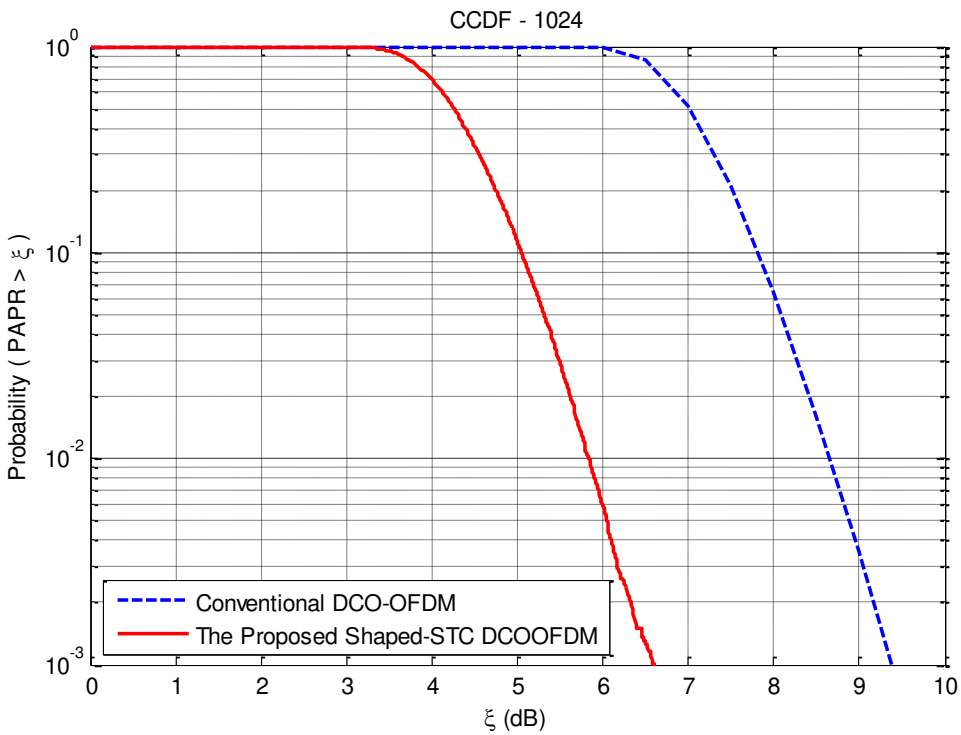

Figure 16. The PAPR performance of the proposed shaped STC-DCOOFDM system.

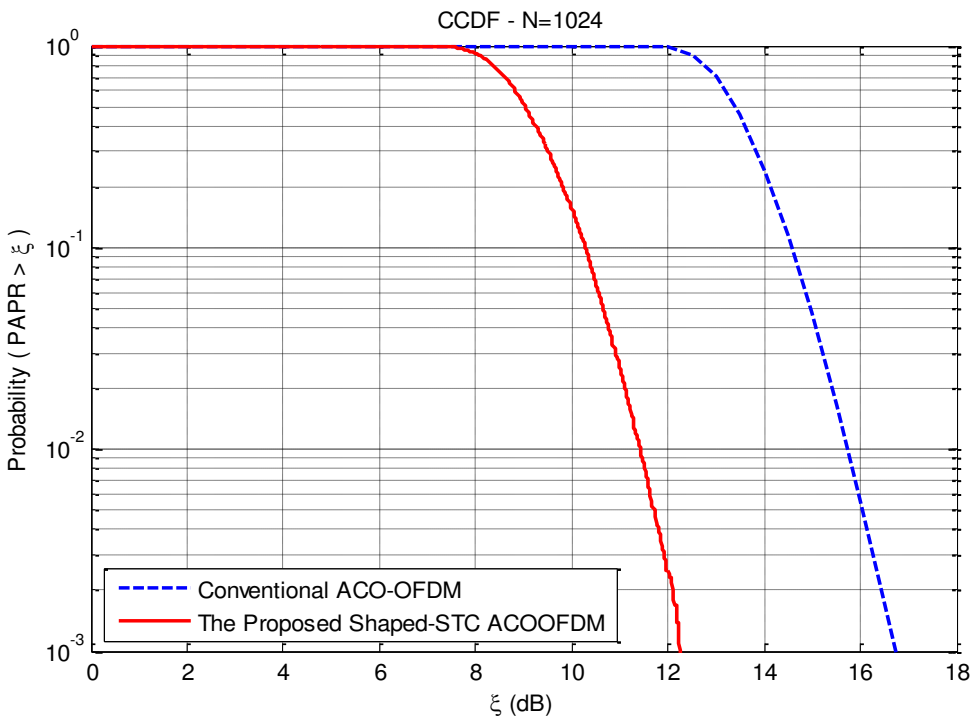

Figure 17. The PAPR performance of the proposed shaped STC-ACOOFDM system.

The PAPR performance of the proposed shaped STC-ACOOFDM system is demonstrated in Figure 17. It is easy to notice that the results are similar to those results in Figure 16. At CCDF=10^{-1}, the PAPR of the proposed scheme is about 4 dB which is a smaller amount of the conventional ACO-OFDM system. TABLE II summarizes the PAPR values of standard optical OFDM and the proposed techniques.

Now, we will show the BER improvement for DCO-OFDM and ACO-OFDM systems using the proposed scheme. Figure 18 and Figure 19 demonstrate the BER outcomes for DCO-OFDM system with 7 dB bias and ACO-OFDM system, respectively.

TABLE II

PAPR evaluation at CCDF=0.1

Ssytem types / PAPR	ξ (dB)	Power Saving (dB)
DCO-OFDM	8	5.22
The Proposed STC-DCOOFDM	5.22	
ACO-OFDM	14.5	4.29
The Proposed STC-ACOOFDM	10.21	

Now, we will show the BER improvement for DCO-OFDM and ACO-OFDM systems using the proposed scheme. Figure 18 and Figure 19 demonstrate the BER outcomes for DCO-OFDM system with 7 dB bias and ACO-OFDM system, respectively.

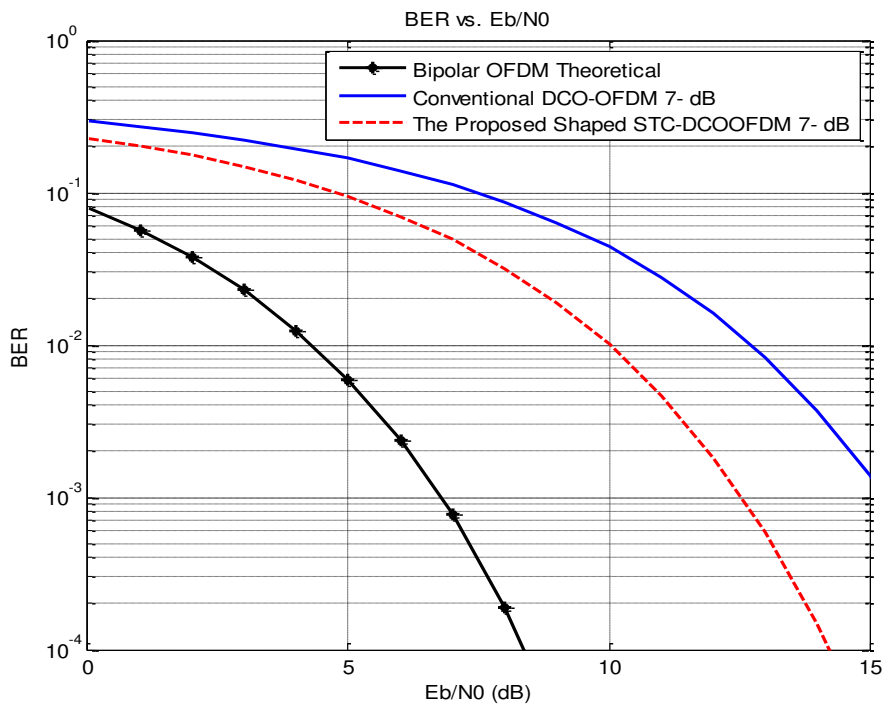

Figure 18. BER performance of the proposed shaped STC-DCOOFDM system.

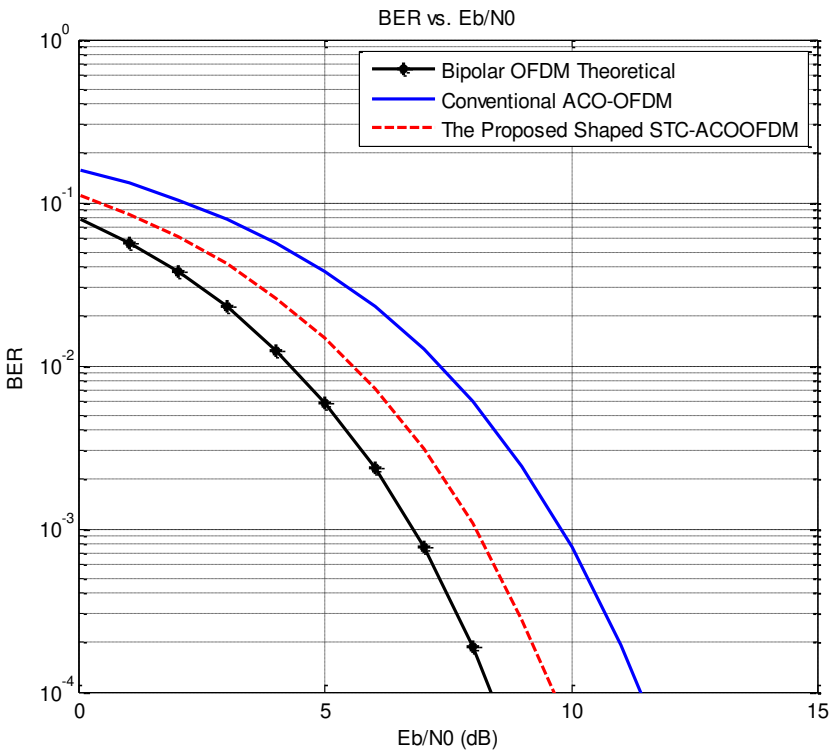

Figure 19. BER performance of the proposed shaped STC-ACOOFDM system.

These figures compare the BER before and after applying the proposed scheme. As shown from Figure 18, the proposed shaped STC-DCOOFDM scheme achieves 10^{-3} BER at 12 dB but the traditional DCO-OFDM system achieves that value of BER at 15 dB. Hence, the proposed shaped STC-DCOOFDM scheme improves the power requirement by 3 dB compared to traditional DCO-OFDM system. Furthermore, the proposed shaped STC-ACOOFDM system attains BER performance at 8 dB but the traditional ACO-OFDM at about 9.5 dB as shown in Figure 19. Thus, the proposed shaped STC-ACOOFDM system enhances the power requirement by about 1.5 dB compared to traditional ACO-OFDM system.

VI. Conclusions

In this study, the proposed shaped STC-DCO-OFDM system and the suggested shaped STC-ACO-OFDM system are compared to typical DCO-OFDM and ACO-OFDM systems in terms of spectrum efficiency, OOB, PAPR, power savings, computational complexity, and BER. Traditional systems have the same spectral efficiency as the suggested systems. When compared to DCO-OFDM and

ACO-OFDM systems, the suggested strategies exhibit a low PAPR and considerable power savings. Furthermore, as compared to existing systems, the suggested methods lessen the OOB notion. Furthermore, the suggested systems have a reduced computational complexity than DCO-OFDDM systems. Finally, the suggested systems outperform existing systems for the BPSK scheme in the AWGN environment in terms of BER performance.

REFERENCES

[1] Cisco Visual Networking Index. (Feb. 2016). Global Mobile Data Traffic Forecast Update, 2015_2020. [Online]. Available: http://www. cisco.com/c/en/us/solutions/collateral/service-provider.pdf

[2] A. Jovicic, J. Li, and T. Richardson, ``Visible light communication: Oppor- tunities, challenges and the path to market," IEEE Commun. Mag., vol. 51, no. 12, pp. 26_32, Dec. 2013.

[3] M. Z. Chowdhury, M. T. Hossan, A. Islam, and Y. M. Jang, ``A comparative survey of optical wireless technologies: Architectures and applications," IEEE Access, vol. 6, pp. 9819_9840, Jan. 2018.

[4] J. Armstrong, ``OFDM for optical communications," J. Lightw. Technol., vol. 27, no. 3, pp. 189_204, Feb. 1, 2009.

[5] J. Gancarz, H. Elgala, and T. D. C. Little, ``Impact of lighting requirements on VLC systems," IEEE Commun. Mag., vol. 51, no. 12, pp. 34_41, Dec. 2013.

[6] Dissanayake, S.D.; Armstrong, J. Comparison of ACO-OFDM, DCO-OFDM and ADO-OFDM in IM/DD Systems. J. Lightwave Technol. 2013, 31, 1063–1072.

[7] Armstrong, J.; Schmidt, B.J.C. Comparison of Asymmetrically Clipped Optical OFDM and DC-Biased Optical OFDM in AWGN. IEEE Commun. Lett. 2008, 12, 343–345.

[8] A. Farhang, N. Marchetti, F. Figueiredo, and J. P. Miranda, “Massive MIMO and Waveform Design for 5th Generation Wireless Communication Systems,” Proc. Int. Conf. on 5G for Ubiq. Connectivity, pp. 70–75, Nov. 2014.

[9] V. Vakilian, T. Wild, F. Schaich, S. Brink, and J. F. Frigon, “Universalfiltered Multi-carrier Technique for Wireless Systems Beyond LTE,” Proc. 2013 GC Wkshps, pp. 223–228, Dec. 2013.

[10] H. Kuriki, K. Mizutani, T. Matsumura, and H. Harada, “Enhanced UFOFDM or Long-delay Multipath Fading Environment,” IEEE VTC2017-Spring, pp. 1–5, Jun. 2017.

[11] A. Goldsmith, Wireless Communications, 1st Ed. New York, NY, USA: Cambridge Univ. Press, 2005.

[12] H. Ochiai and H. Imai, “on the distribution of the peak-to-average power ratio in OFDM signals," IEEE Trans. Commun., vol. 49, no. 2, pp. 282_289, Feb. 2001.

[13] S. H. Han and J. H. Lee, “An overview of peak-to-average power ratio reduction techniques for multicarrier transmission," IEEE Wireless Commun., vol. 12, no. 2, pp. 56_65, Apr. 2005.

[14] N. Jacklin and Z. Ding, ``A linear programming based tone injection algorithm for PAPR reduction of OFDM and linearly precoded systems," IEEE Trans. Circuits Syst. I, Reg. Papers, vol. 60, no. 7, pp. 1937-1945, Jul. 2013.

[15] J. Wang, Y. Xu, X. Ling, R. Zhang, Z. Ding, and C. Zhao,” PAPR analysis for OFDM visible light communication," Opt. Exp., vol. 24, pp. 27457_27474, Nov. 2016.

[16] H. Chen, J. He, J. Tang, F. Li, M. Chen, and L. Chen, ``Performance of 16 QAM-OFDM with new null subcarrier shifting in an intensity-modulated direct detection system," J. Opt. Commun. Netw. vol. 6, no. 2, pp. 159_164, Feb. 2014.

[17] W. O. Popoola, Z. Ghassemlooy, and B. G. Stewart, ``Pilot-assisted PAPR reduction technique for optical OFDM communication systems," J. Lightw. Technol., vol. 32, no. 7, pp. 1374_1382, Apr. 1, 2014.

[18] J. Hou, X. Zhao, F. Gong, F. Hui, and J. Ge, ``PAPR and PICR reduction of OFDM signals with clipping noise-based tone injection scheme," IEEE Trans. Veh. Technol., vol. 66, no. 1, pp. 222_232, Jan. 2016.

[19] B. Ranjha and M. Kavehrad, ``Hybrid asymmetrically clipped OFDM-based IM/DD optical wireless system," IEEE/OSA J. Opt. Commun. Netw., vol. 6, no. 4, pp. 387–396, Apr. 2014.M.

[20] Mohamed S. Elbakry, et al. "A symbol time compression for ICI reduction in high mobility OFDM systems." 2017 29th International Conference on Microelectronics (ICM). IEEE, 2017.
[21] Mohamed S. Elbakry, et al. "A time inversion and symbol time compression (TI-STC) scheme for ICI cancellation in high mobility OFDM systems." 2017 Japan-Africa Conference on Electronics, Communications and Computers (JAC-ECC). IEEE, 2017.
[22] M. Y. I. Afifi, et al. “An efficient technique for out-of-band power reduction for the eliminated CP-STC-shaped system for 5g requirements, International Journal of Electrical and Computer Engineering 10 (5) (2020) 5306.
[23] M. Y. I. Afifi,, et al. “An Efficient Performance of OFDM-Shaped Symbol for 5G Green Communication Compared to FBMC”, Advances in Science, Technology and Engineering Systems Journal (ASTESJ), Volume 5, Issue 6, Page No 1163-1170, 2020
[24] Bhadoria, Mahendra PS, Gaurav Pandey, and Abhishek Dixit. "Performance evaluation of visible light communication for DCO and ACO optical OFDM techniques." 2019 National Conference on Communications (NCC). IEEE, 2019.
[25] Mossaad, Mohammed. "Theoretical analysis and simulation of IM/DD optical OFDM systems." McMaster Universit, URL: http://www. Academia. Edu/19322099 (2011).
[26] Sobhy, Androw, et al. "Enhancing the performance of optical VLC system based on asymmetric symmetric subcarriers OFDM." International Journal of Communication Systems 33.10 (2020): e4226.
[27] You, Xiaodi, et al. "Time domain reshuffling for OFDM based indoor visible light communication systems." Optics express 25.10 (2017): 11606-11621.
[28] Mesleh, Raed, Hany Elgala, and Harald Haas. "On the performance of different OFDM based optical wireless communication systems." IEEE/OSA Journal of Optical Communications and Networking 3.8 (2011): 620-628.
[29] Jayalath, A. Dhammika S., and Chintha Tellambura. "Reducing the out-of-band radiation of OFDM using an extended guard interval." IEEE 54th Vehicular Technology Conference. VTC Fall 2001. Proceedings (Cat. No. 01CH37211). Vol. 2. IEEE, 2001.
[30] Gallo, Rodaina GA, et al. "Real-DFT Based DCO-OFDM and ACO-OFDM for Optical Communications Systems." 2019 21st International Conference on Transparent Optical Networks (ICTON) IEEE, 2019.
[31] Ahmad, Rizwana, and Anand Srivastava. "PAPR Reduction of OFDM Signal Through DFT Precoding and GMSK Pulse Shaping in Indoor VLC." IEEE Access 8 (2020): 122092-122103.